

Original Paper

Effect of Illuminated Light Wavelength on Electric Resistance of Zinc Oxide Films Prepared by Spin-Spray Method

Hajime WAGATA^{1,*}, Naoki OHASHI², Ken-ichi KATSUMATA³, Kiyoshi OKADA³
Nobuhiro MATSUSHITA³, Shuji OISHI¹, Katsuya TESHIMA¹

¹Department of Environmental Science and Technology, Faculty of Engineering, Shinshu University
4-17-1 Wakasato, Nagano 380-8553

²National Institute for Materials Science (NIMS), 1-1 Namiki, Tsukuba 305-0044

³Materials and Structures Laboratory, Tokyo Institute of Technology, 4259 Nagatsuta, Midori
Yokohama 226-8503

Received September 19, 2012; E-mail: wagata@shinshu-u.ac.jp

Decrease of electric resistance during light-illumination was observed in ZnO films prepared by a low-temperature (< 100 °C) wet-chemical process. The electric resistance was measured by 2-terminal method, and decreased from 2 MΩ to 200 Ω by UV illumination for 12 h. The decrease of the resistance was strongly affected by the light wavelength, showing that the ZnO film illuminated by the light with shorter wavelength (365 nm) had lower electric resistance compared to the others (380, and 420 nm). In contrast, light with wavelength of 365 nm were more effective to maintain the resistance compared to that with wavelength of 325 nm. It indicated that the penetration depth of the light in the films were also important to decrease the resistance of the films.

Key Words: ZnO, Thin Film, Spin-Spray Method, Aqueous Solution Method, Transparent Conductive Electrode

1. Introduction

The film fabrication techniques for functional ceramics can be generally classified into vapor phase and liquid phase method depending on the chemical states of raw materials. The vapor phase method includes physical vapor deposition (PVD) and chemical vapor deposition (CVD), and uses vaporized raw materials for fabrication of the films. In contrast, liquid phase method is often considered as chemical solution deposition (CSD) probably due to few kinds of physical liquid phase deposition. Some of these methods are necessary to be prepared by substrate heating and/or post-preparation heating of above several hundred °C for the crystallization. Although the heat-treatment has offered high quality metal oxide films, the development of low-temperature syntheses is valuable for not only lower environmental load and energy consumption[1] but also applying to flexible electronics utilizing functional polymers which are not tolerable to high-temperature.

There are growing interests for solution processes to achieve functional metal oxide films because of the above advantages. Aqueous solution methods including hydrothermal, electrochemical, electroless deposition and chemical bath deposition (CBD) are promising methods to fabricate films due to their low manipulating temperatures under 100 °C. These methods have provided opportunities to exploit excellent properties due to the unique nano/micro-structures and explore possible novel phenomena arising from the structures. In particular, various inorganic semiconductor films with unique nano/micro-structures have been investigated for their potential usages to the industry. Zinc oxide (ZnO) is one of semiconductor materials and is expected to offer various practical uses such as ultraviolet lasing[2], field emission devices[3], gas sensors[4], photocatalysts[5], hydrophilic-hydrophobic converting surface[6], transparent conducting electrode[7], piezoelectric devices[8] and thin film transistors[9]. Preparation of ZnO films by using aqueous chemistry have been researched intentionally because anisotropic crystal growth of ZnO in solution and controllability of the growth rate using structure-directing agent have enabled us to make unique and special architectures.

Recently, our group has succeeded to fabricate transparent ZnO films with electric resistivity of $4.4 \times 10^{-3} \Omega\cdot\text{cm}$ by spin-spray method and subsequent UV treatment[10]. Spin-spray method is a promising aqueous solution method, and mainly has been developed for the preparation of spinel ferrite films[11-14]. The scheme of the spin-spray technique is shown in Fig.1. The both a source solution containing metal salt and a reaction solution containing pH adjuster/additives are simultaneously sprayed onto substrates mounted on a temperature-controlled rotating table. The principle of the chemical reaction is the same as that of CBD. However, the spin-spray technique has been shown to have several advantages for making metal oxide films, including high crystal quality and a high deposition rate ($\sim 100 \text{ nm}\cdot\text{min}^{-1}$) to make a thick film ($\sim 10 \mu\text{m}$). These advantages have been attributed to the following characteristics; one is solution flow caused by centrifugal force, which removes free nuclei formed in the solution and results in selective growth of nuclei bounded on substrate. The other is continuous supply of fresh solution, which maintains the high

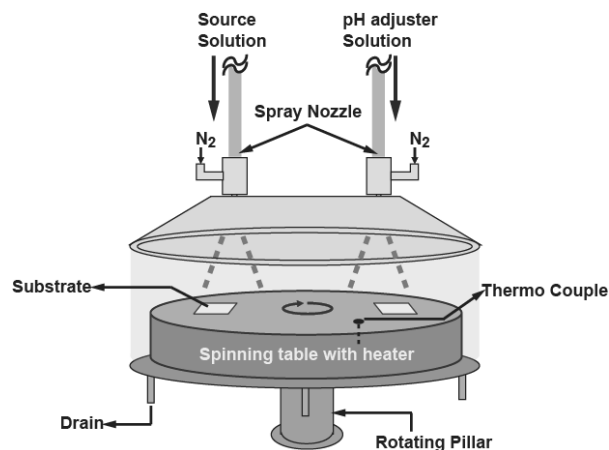


Fig.1 Schematic illustration of spin-spray equipment.

concentration of solute and results in thick films with a high deposition rate. These features are appropriate for non-seeded deposition of high-quality ZnO films through the chemical route. Although the ZnO films fabricated by spin-spray method showed visible-light transparency over 75 % [15], their electric resistivity were too high ($> 10 \Omega \cdot \text{cm}$) for the practical applications. The subsequent UV treatment after the fabrication of the films drastically decreased the resistivity because the decomposition of residual organic species in the films induced dopants such as hydrogen and carbon species, and oxygen defects in ZnO lattice [10]. Although the permanent decrease in the resistivity was estimated to be caused by the penetration of UV light in the films, the subsequent treatment was conducted by using only a commercial UV lamp with a broad emission wavelength. Therefore more detail analysis on the effect of light wavelength was required to understand the mechanisms of the light-illumination treatment.

Herein, we report the change in electric resistance of the spin-sprayed ZnO films by light illumination with various emission wavelengths. The result indicated that the light wavelength and the penetration of light in the films were important factor for maintaining the decreased electric resistance.

2. Experimental

2.1 Fabrication of ZnO Film by Spin-Spray Method

Zinc nitrate hexahydrate (Wako Pure Chemical Industries, Ltd., Japan, 99.0 %) aqueous solution and ammonia water (Wako Pure Chemical Industries, Ltd., Japan, 28.0 %) with trisodium citrate (Wako Pure Chemical Industries, Ltd., Japan, 97.0 %) were used as received. Millipore deionized water was used for preparing the solutions. The $\text{Zn}(\text{NO}_3)_2$ aq was prepared by dissolving 10 mmol of zinc nitrate in 1.00 L of deionized water. The dilute ammonia was prepared by dissolving 60 mL of ammonia water in 0.94 L of deionized water. Trisodium citrate was added to the dilute ammonia to prepare 2.0 mM of citrate solutions. The pH of the source solution was 7.0 whereas the pH of the pH modifier was 12.0 without citrate and 11.6 – 11.7 with citrates. The pH of the solution after the reaction was 10.5 without citrate and 10.1 – 10.2 with citrates. The reaction was performed under flowing N_2 ($1.0 \text{ L} \cdot \text{min}^{-1}$) with continuous stirring to prevent the pH change by dissolving of CO_2 and O_2 from an atmosphere.

A soda-lime glass substrate ($40 \times 30 \times 0.17 \text{ mm}^3$) were washed in an ultrasonic bath with Millipore deionized water and ethanol for 10 min each. The rinsed substrate was exposed to glow discharge plasma for 5 min to obtain a hydrophilic surface. The surface modified substrates were mounted on a temperature controlled rotating table. The temperature and rotation rate of the table were set to $90 \text{ }^\circ\text{C}$ and 120 rpm, respectively. The source solution and pH modifier were simultaneously sprayed onto the substrates through an each nozzle using diaphragm pumps. The supply rates of the source solution and pH modifier were each set to $3.0 \text{ L} \cdot \text{h}^{-1}$, thus, the total supply rate was $6 \text{ L} \cdot \text{h}^{-1}$. The details of the experimental setup are described elsewhere [15,16]. The total deposition time was set to 10 min. All samples were dried at $100 \text{ }^\circ\text{C}$ for 1 day to eliminate the adsorbed water.

2.2 Light-Illumination Treatment on the Spin-Sprayed ZnO Films

Firstly, a black-light-blue (BLB) lamp was used as UV light source, which has the wavelength of 300 – 400 nm with maximum emission at near 360 nm and the intensity of $2.0 \text{ mW} \cdot \text{cm}^{-2}$ (FL8BLB, Toshiba Lighting & Technology Co., Ltd., Japan), as measured by a UV light meter (UV-340, Custom Co., Ltd., Japan). An optical module with Xenon lamp (UXL-300SX, Ushio Inc., Japan) was used to evaluate the effect of the wavelength. Various wavelengths of 365, 380, and 400 nm with the intensities of 30, 24, and $40 \mu\text{W} \cdot \text{cm}^{-2}$ respectively were generated by conducting the light through the grating and band pass filter. Those intensities were measured using optical power meters [Q8230 for $\lambda = 400 \text{ nm}$

(Advantest Co., Ltd., Japan) and UM-10 for $\lambda = 365$ and 380 nm (Konica Minolta Sensing Inc., Japan)]. A He-Cd laser (Kimmon Koha Co., Ltd.) with center wavelength of 325 nm and intensity of $3.4 \text{ mW} \cdot \text{cm}^{-2}$ and a light emitting diode (LED, NCSU033A, Nichia Co., Ltd., Japan) with center wavelength of 365 nm and intensity of $3.0 \text{ mW} \cdot \text{cm}^{-2}$ were also used as the light sources. The irradiation time was 0 to 1200 min. All the light-illumination experiments were performed at room temperature and ambient atmosphere.

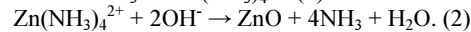
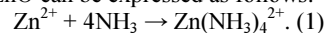
2.3 Characterization

The crystalline phases of the deposited films were identified by X-ray diffraction (XRD) θ - 2θ scan using a MiniflexII (Rigaku Corp., Japan) with Cu $K\alpha$ radiation ($\lambda = 0.154 \text{ nm}$). The surface and cross-sectional structures of the films were observed with a scanning electron microscope (SEM, S4000, Hitachi Co., Ltd., Japan). The thickness of the films was measured from the cross-sectional images of SEM. The optical transmittance of the films in the UV-visible (UV-Vis) range by UV illumination was monitored with a Lambda 35 spectrometer (Perkin Elmer Japan Co., Ltd.). The electric resistance of the films were measured by 2-terminal with digital multi-meter, and the distance of the each termination is set at 10 mm.

3. Result & Discussion

3.1 Microstructure & Crystal Phase

Figure 2 (a) shows the surface and cross-sectional SEM images of the as-prepared ZnO films spin-sprayed for 10 min using trisodium citrate. No pores and cracks were observed in the films. Figure 2 (b) shows the XRD patterns of the ZnO film. It indicated that the crystal phase of the obtained film was identified to ZnO with wurtzite-type crystal structure (ICDD PDF 36-1451). We assumed that most of the Zn ions formed $\text{Zn}(\text{NH}_3)_4^{2+}$ complex in the thin liquid film on the substrate from the speciation diagrams of soluble zinc species [17,18]. Accordingly, the reaction for forming ZnO can be expressed as follows:



Such a reaction occurs in a solution at elevated temperature [18,19] and results in the formation of ZnO films. The average thickness of the ZnO films fabricated in this condition was $1.05 \mu\text{m}$. The thickness of the films were 1.21, 1.08, 1.02, 0.90, 1.10 and $1.06 \mu\text{m}$ for those treated by BLB lamp, Xenon with 360 nm, 380 nm, and 400 nm, LED with 365 nm, and He-Cd laser with 325 nm, respectively.

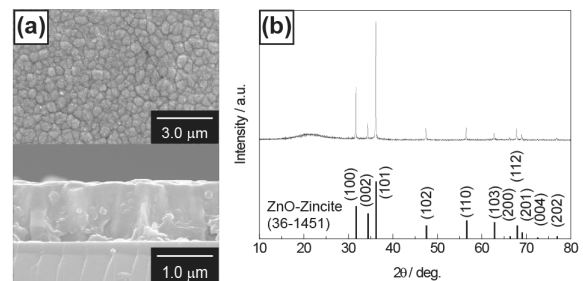


Fig.2 (a) Surface and cross-sectional SEM images and (b) XRD pattern of ZnO film fabricated by spin-spray method.

3.2 Light-Illumination Treatment by BLB Lamp

When the ZnO film was set in dark for 1 week, the film showed electric resistance of $\sim 2 \text{ M}\Omega$. Under indoor light for several minutes, the electric resistance decreased to about several hundred $\text{k}\Omega$, which is maintained for several days even in dark. After UV light-illumination by a BLB lamp, the electric resistance of the film

drastically decreased as shown in Fig.3. After UV light illumination for 60 min, the electric resistance decreased three digits to 600 Ω. Longer UV light illumination resulted in gradual decrease in the electric resistance and finally they reached to 200 Ω by illumination for 1200 min. When a semiconductor absorbs light with energy higher than the band gap energy, electron-hole pairs are generated according to eq. (3)

$$h\nu \rightarrow h^+ + e^- \quad (3)$$

It effectively results in the increase of electric conduction with solid-state process for the photoconduction of conventional semiconductors. The electron and holes generated by light absorption rapidly vanish after turning off the light. Therefore, the photoresponse, namely, rises in conductivity upon light illumination and the decay after cutting off light due to the solid-state process, is expected to be very rapid[20,21]. In contrast, in case of the spin-sprayed ZnO films, the electric resistance was not recovered to the initial value. It is reasonable to consider that this phenomenon does not only originate from increase of temporal carriers under light-illumination but also the other effect relevant to increase in intrinsic carriers in ZnO crystals.

Figure 4 shows optical absorption edge of the light-illuminated ZnO films. The optical band gap of the films is determined by applying the following equation in high absorbance region[22];

$$(ah\nu)^2 = C(E_g - h\nu) \quad (4)$$

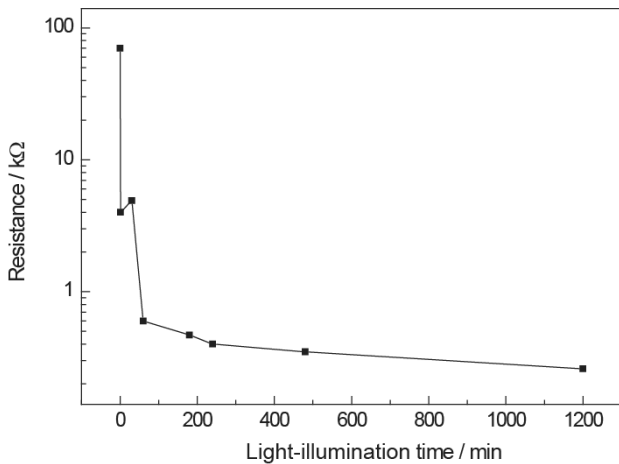


Fig.3 Change in the electric resistance of the ZnO films by light-illumination treatment with a BLB lamp.

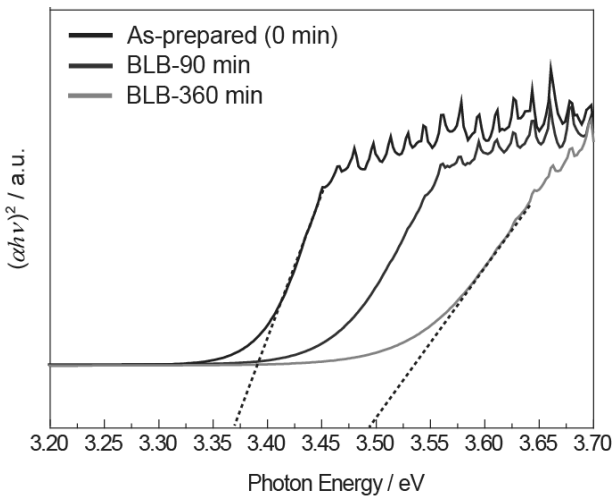


Fig.4 Optical absorption edge of the ZnO films after BLB illumination for different times.

Where a is the absorption coefficient, h is the Planck's constant, ν is the frequency of photon, $h\nu$ is the energy of the photon, E_g is the optical band gap, and C is a constant. The E_g value can be obtained by extrapolating the linear portion to the photon energy axis in the figure. The E_g value of the as-deposited ZnO films was 3.38 eV; consequently, they could absorb UV light during the light-illumination treatment because the BLB lamp had a central wavelength of 360 nm ($h\nu = 3.44$ eV). The optical band gap shifted gradually to a higher value, reaching 3.49 eV after 360 min of UV treatment. This movement of the band gap is often observed in other-metal-ion doped ZnO with high electron concentration[23,24] and explained by the cause of the Burstein-Moss (BM) shift[25], an energy band widening (blue shift) effect resulting from the increase of the Fermi level in the conduction band of degenerate semiconductors. The both results indicated that the carrier concentration of the film estimated to be increased by light-illumination treatment. In fact, the increasing carrier concentration and decomposition of organics were observed at the same time in the previous study[10].

3.3 Effect of Wavelength on Electric Resistance of the ZnO Films

Since the decreased resistance was maintained and did not recover (increase) to the initial value even in dark in ambient atmosphere, the change in the resistance were estimated to be mainly originated from permanent changes in ZnO because usual rapid increase and decrease of conductivity by light illumination is mainly caused by the sorption and desorption of gaseous species on the surface and grain boundaries[20,21,26]. Considering this assumption, some of defects in ZnO crystals which can be excited by visible light may contribute to the decreased electric resistance and penetration of visible light all over the films may cause increase of carriers all over the films. Djuricic et al.[27] reported that red-orange luminescence of solution-processed ZnO was enhanced by near UV light (~420 nm) excitation which was smaller than the band gap energy of ZnO. It indicated that several defect levels could exist in intra band of ZnO crystals. To determine the effect, the lights with various wavelengths at 365, 380, and 400 nm were generated and illuminated at the samples. Since the optical band gap of as-prepared samples were around 3.37 eV, light with the wavelengths at 380 and 400 nm will not excite electrons from the valence band to the conduction band due to lower energy than band gap. Figure 5 shows the change in electric resistance of the ZnO film after illumination of the light with various wavelengths

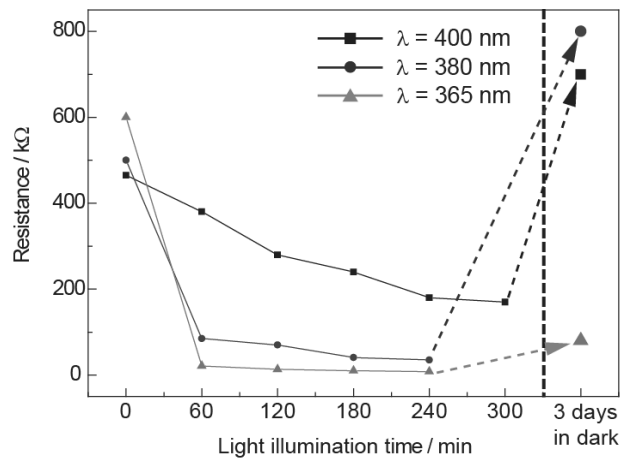


Fig.5 Time dependence of the electric resistances of the ZnO film during light illumination with wavelengths at 365, 380 and 400 nm. "3 days in dark" in this figure means that the samples were set in dark for three days at R.T. in ambient pressure.

depending on the illumination time. The light-illumination decreased electric resistance of the ZnO film in all conditions. Shorter the light wavelength caused lowering of the electric resistance. After dark storage for three days, the electric resistance of the light illuminated films increased. In case of wavelengths at 380 and 400 nm, the electric resistances recovered closely to the initial value after dark storage for three days. Although the light illumination with wavelength at 365 nm also showed slight increase of electric resistance in dark, it was fairly low compared with the initial value. Since the calculated photon numbers by illumination of wavelengths at 365, 380 and 400 nm are 1.1×10^{18} , 6.6×10^{17} and 1.1×10^{18} , respectively, the phenomenon does not strongly depend on the photon numbers but on the wavelength of the light. The light with higher energy than the band gap was effective for keeping the long-term low electric resistance of the ZnO film. In addition, recovery (increase) of resistance by dark storage indicates the existence of temporal carriers induced by light illumination.

To confirm the effect of wavelength under band edge of the ZnO films, a He-Cd laser with wavelength at 325 nm and a LED with wavelength at 365 nm were used. The irradiation time was 240 min and total photon numbers were 8.1×10^{19} for the He-Cd laser and 7.9×10^{19} for the LED. Figure 6 shows the change in electric resistances of the ZnO film after light illumination and dark storage. The both light-illuminated samples showed similar electric resistances of approximately 1.0 k Ω . After the light illumination, the samples were set in dark and the electric resistances gradually increased. The sample illuminated at 365 nm have slower increasing rate of the electric resistance than that at 325 nm. After 50 days in dark, sample illuminated at 325 nm showed electric resistance close to the initial value whereas that at 365 nm still exhibited lower electric resistance than the initial value. Since the photon numbers of both light sources were almost same and the light energies exceeded the band gap energy of the samples (~ 3.37 eV), light with wavelength at 365 nm was realized to be more effective for slow decay of electric conductivity than that at 325 nm. It can be interpreted by the different light penetration depths: the light at 325 nm (3.81 eV) only reacts with the surface of the ZnO films with the penetration depth of approximately 60 nm (calculated from absorbance of ZnO film fabricated on *c*-plane sapphire substrate[28], and Beer-Lambert law), whereas the light at 365 nm (3.40 eV) can penetrate through the film because the band gap of the ZnO films gradually increased by increasing illumination time (see Fig.4). Namely, the light at 365 nm can react

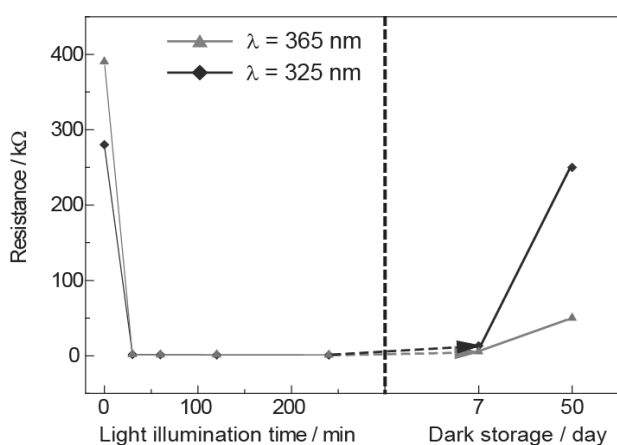


Fig.6 Time dependence of the electric resistances of the ZnO film during light illumination with wavelengths at 325 nm (He-Cd laser) and 365 nm (LED). Change in the electric resistances after dark storage at R.T. in ambient atmosphere is shown in the right side of this figure.

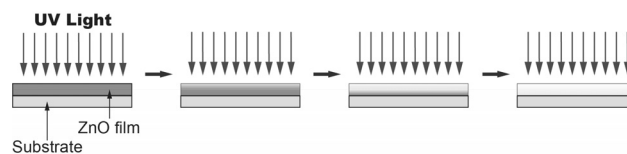


Fig.7 Schematic illustration for penetration of light through the entire ZnO film. The blue and white indicates non-irradiated and irradiated region, respectively.

with all the region of the samples whereas the light at 325 nm can only react with the surface of the samples.

The schematic illustration of light-penetration is shown in Fig.7. Firstly, light illumination decomposed organic adsorbents on surface of ZnO film and induced carriers at the same time. The band edge of the surface region moved toward higher energy side by BM shift. Then, UV light penetrates through the surface and absorbed by inner region of the film, where electron carriers have not increased yet. Finally, UV light penetrates through all the region of the films and organics will be totally decomposed. In fact, UV light illumination from the opposite (substrate) side of the film causes same effect, which is an evidence of UV light penetration through the films.

4. Summary

The post-deposition light-illumination treatment was performed to the spin-sprayed ZnO films. The electric resistance of the spin-sprayed ZnO film was decreased by UV light-illumination treatment from 2 M Ω to 200 Ω by UV illumination for 12 h. The wavelength of the light strongly affected the decrease of the resistance. The light with wavelength of 365 nm was more effective than those with 380 and 400 nm, indicating that light with higher energy (shorter wavelength) was more effective to decrease the resistance. In addition, it was found that the light wavelength should be properly selected because a LED with wavelength of 365 nm was more effective to maintain the decreased resistance than He-Cd laser with wavelength of 325 nm. In case of the wavelength of 365 nm, the penetration of the light in deeper region of the film was considered due to change in the optical bandgap. Namely, it indicated that the penetration depth of the light competing with the change in the optical bandgap of ZnO was important to decrease the resistance.

Acknowledgment

This research was partially supported by a Grant-in-Aid for Young Scientists (Start-up) (No.24860031) from Japan Society for the Promotion of Science (JSPS). The authors gratefully thank to Dr. Hiroyo Segawa and Dr. Yoshiki Wada to help the light-illumination experiments.

References

- 1) M. Yoshimura, *J. Mater. Res.*, **1998**, *13*, 796.
- 2) J. H. Choy, E. S. Jang, J. H. Won, J. H. Chung, D. J. Jang, Y. W. Kim, *Adv. Mater.*, **2003**, *15*, 1911.
- 3) J. Liu, J. C. She, S. Z. Deng, J. Chen and N. S. Xu, *J. Phys. Chem. C*, **2008**, *112*, 11685.
- 4) T. J. Hsueh, C. L. Hsu, S. J. Chang, I. C. Chen, *Sensors and Actuators B-Chemical*, **2007**, *126*, 473.
- 5) Y. Liu, Z. H. Kang, Z. H. Chen, I. Shafiq, J. A. Zapien, I. Bello, W. J. Zhang, S. T. Lee, *Cryst. Growth & Des.*, **2009**, *9*, 3222.
- 6) X. J. Feng, L. Feng, M. H. Jin, J. Zhai, L. Jiang, D. B. Zhu, *J. Am. Chem. Soc.*, **2004**, *126*, 62.

- 7) T. Minami, *Semicond. Sci. Technol.*, **2005**, *20*, S35.
- 8) M. Y. Choi, D. Choi, M. J. Jin, I. Kim, S. H. Kim, J. Y. Choi, S. Y. Lee, J. M. Kim, S. W. Kim, *Adv. Mater.*, **2009**, *21*, 2185.
- 9) S. T. Meyers, J. T. Anderson, C. M. Hung, J. Thompson, J. F. Wager, D. A. Keszler, *J. Am. Chem. Soc.*, **2008**, *130*, 17603.
- 10) H. Wagata, N. Ohashi, K. Katsumata, H. Segawa, Y. Wada, H. Yoshikawa, S. Ueda, K. Okada and N. Matsushita, *J. Mater. Chem.*, **2012**, *22*, 20706.
- 11) M. Abe, Y. Tamaura, *J. Appl. Phys.*, **1984**, *55*, 2614.
- 12) M. Abe, *MRS Bull.*, **2000**, *25*, 51.
- 13) S. K. Ailoor, T. Taniguchi, K. Kondo, M. Tada, T. Nakagawa, M. Abe, M. Yoshimura, N. Matsushita, *J. Mater. Chem.*, **2009**, *19*, 5510.
- 14) M. Liu, O. Obi, J. Lou, Y. J. Chen, Z. H. Cai, S. Stoute, M. Espanol, M. Lew, X. Situ, K. S. Ziemer, V. G. Harris and N. X. Sun, *Adv. Funct. Mater.*, **2009**, *19*, 1826.
- 15) H. Wagata, N. Ohashi, T. Taniguchi, K. I. Katsumata, K. Okada, N. Matsushita, *Cryst. Growth & Des.*, **2010**, *10*, 4968.
- 16) H. Wagata, N. Ohashi, T. Taniguchi, A. K. Subramani, K. Katsumata, K. Okada, N. Matsushita, *Cryst. Growth & Des.*, **2010**, *10*, 3502.
- 17) I. Rodriguez-Torres, G. Valentin, F. Lopicque, *J. Appl. Electrochem.*, **1999**, *29*, 1035.
- 18) C. Hubert, N. Naghavi, B. Canava, A. Etcheberry, D. Lincot, *Thin Solid Films*, **2007**, *515*, 6032.
- 19) Y. Tak, K. J. Yong, *J. Phys. Chem. B*, **2005**, *109*, 19263.
- 20) Y. Takahashi, M. Kanamori, A. Kondoh, H. Minoura, Y. Ohya, *Jpn. J. Appl. Phys.*, **1994**, *33*, 6611.
- 21) S. A. Studenikin, N. Golego, M. Cocivera, *J. Appl. Phys.*, **2000**, *87*, 2413.
- 22) K. F. Berggren, B. E. Sernelius, *Phys. Rev. B*, **1981**, *24*, 197.
- 23) J. G. Lu, Z. Z. Ye, Y. J. Zeng, L. P. Zhu, L. Wang, J. Yuan, B. H. Zhao, Q. L. Liang, *J. Appl. Phys.*, **2006**, *100*, 073714.
- 24) O. Bamiduro, H. Mustafa, R. Mundle, R. B. Konda, A. K. Pradhan, *Appl. Phys. Lett.*, **2007**, *90*, 252108.
- 25) E. Burstein, *Phys. Rev.*, **1954**, *93*, 632.
- 26) Y. Z. Jin, J. P. Wang, B. Q. Sun, J. C. Blakesley, N. C. Greenham, *Nano Lett.*, **2008**, *8*, 1649.
- 27) A. B. Djuricic, Y. H. Leung, K. H. Tam, Y. F. Hsu, L. Ding, W. K. Ge, Y. C. Zhong, K. S. Wong, W. K. Chan, H. L. Tam, K. W. Cheah, W. M. Kwok, D. L. Phillips, *Nanotechnol.*, **2007**, *18*, 095702.
- 28) J. F. Muth, R. M. Kolbas, A. K. Sharma, S. Oktyabrsky, and J. Narayan, *J. Appl. Phys.* **1999**, *85*, 7884.